



HAL
open science

Working day and night: plastid casein kinase 2 catalyses phosphorylation of proteins with diverse functions in light- and dark-adapted plastids

Anja Rödiger, Johann Galonska, Elena Bergner, Birgit Agne, Stefan Helm, Saleh Alseekh, Alisdair R Fernie, Domenika Thieme, Wolfgang Hoehenwarter, Gerd Hause, et al.

► To cite this version:

Anja Rödiger, Johann Galonska, Elena Bergner, Birgit Agne, Stefan Helm, et al.. Working day and night: plastid casein kinase 2 catalyses phosphorylation of proteins with diverse functions in light- and dark-adapted plastids. *Plant Journal*, 2020, 104 (2), pp.546-558. 10.1111/tpj.14944 . hal-02974315

HAL Id: hal-02974315

<https://hal.science/hal-02974315>

Submitted on 9 Jun 2021

HAL is a multi-disciplinary open access archive for the deposit and dissemination of scientific research documents, whether they are published or not. The documents may come from teaching and research institutions in France or abroad, or from public or private research centers.




L'archive ouverte pluridisciplinaire **HAL**, est destinée au dépôt et à la diffusion de documents scientifiques de niveau recherche, publiés ou non, émanant des établissements d'enseignement et de recherche français ou étrangers, des laboratoires publics ou privés.



Distributed under a Creative Commons Attribution 4.0 International License

RESOURCE

Working day and night: plastid casein kinase 2 catalyses phosphorylation of proteins with diverse functions in light- and dark-adapted plastids

Anja Rödiger¹, Johann Galonska¹, Elena Bergner¹, Birgit Agne¹, Stefan Helm¹, Saleh Alseekh² , Alisdair R. Fernie² ,
Domenika Thieme³, Wolfgang Hoehenwarter³, Gerd Hause⁴, Thomas Pfannschmidt^{5,†} and Sacha Baginsky^{1,*‡} 

¹Institute of Biochemistry and Biotechnology, Martin-Luther-University Halle-Wittenberg, Charles Tanford Proteinzentrum, Kurt-Mothes-Str. 3a, Halle (Saale) 06120, Germany,

²Max-Planck-Institut für Molekulare Pflanzenphysiologie, Wissenschaftspark Golm, Potsdam 14476, Germany,

³Leibniz-Institut für Pflanzenbiochemie, Weinbergweg 3, Halle (Saale) 06120, Germany,

⁴Biocentre, Martin-Luther-University Halle-Wittenberg, Weinbergweg 22, Halle (Saale) 06120, Germany, and

⁵Univ. Grenoble-Alpes, CNRS, CEA, INRA, BIG-LPCV, Grenoble 38000, France

Received 8 August 2019; revised 15 July 2020; accepted 21 July 2020; published online 3 August 2020.

*For correspondence (e-mail sachabaginsky@rub.de).

[†]Present address: Institut für Botanik, Leibniz-Universität Hannover, Herrenhäuserstr. 2, Hannover 30419, Germany

[‡]Present address: Biochemie der Pflanzen, Fakultät für Biochemie und Biotechnologie, Ruhr-Universität Bochum, Universitätsstrasse 150, Bochum, 44801, Germany

SUMMARY

Casein kinase 2 is a ubiquitous protein kinase that has puzzled researchers for several decades because of its pleiotropic activity. Here, we set out to identify the *in vivo* targets of plastid casein kinase 2 (pCK2) in *Arabidopsis thaliana*. Survey phosphoproteome analyses were combined with targeted analyses with wild-type and *pck2* knockdown mutants to identify potential pCK2 targets by their decreased phosphorylation state in the mutant. To validate potential substrates, we complemented the *pck2* knockdown line with tandem affinity tag (TAP)-tagged pCK2 and found it to restore growth parameters, as well as many, but not all, putative pCK2-dependent phosphorylation events. We further performed a targeted analysis at the end-of-night to increase the specificity of target protein identification. This analysis confirmed light-independent phosphorylation of several pCK2 target proteins. Based on the aforementioned data, we define a set of *in vivo* pCK2-targets that span different chloroplast functions, such as metabolism, transcription, translation and photosynthesis. The pleiotropy of pCK2 functions is also manifested by altered state transition kinetics during short-term acclimation and significant alterations in the mutant metabolism, supporting its function in photosynthetic regulation. Thus, our data expand our understanding on chloroplast phosphorylation networks and provide insights into kinase networks in the regulation of chloroplast functions.

Keywords: *Arabidopsis thaliana*, chloroplast, pCK2, phosphorylation, metabolism.

INTRODUCTION

Casein kinase 2 is a ubiquitous protein kinase that has puzzled researchers since its initial isolation from rat liver in 1954. The enzyme is ubiquitously expressed and highly pleiotropic. It phosphorylates numerous substrates, with a striking preference for acidic phosphorylation sites and the consensus phosphorylation motif E/D-S/T-X-E/D-E/D (Pinna, 2002; Salvi *et al.*, 2009). CK2 belongs to the serine threonine kinases, although recent data from mammalian

systems suggested that it can phosphorylate tyrosine residues that are N-terminally localized to aspartic acid *in vivo* and on peptide arrays (Vilk *et al.*, 2008). Intriguingly, the CK2-dependent phosphorylation of a tyrosine residue in histone H2A is responsible for the regulation of transcription elongation, supporting the physiological significance of this unexpected catalytic activity (Basnet *et al.*, 2014). A distinctive feature of CK2 compared to other kinases is the use of both GTP and ATP as a phosphate donor. Interest in CK2 has increased in recent years because of its major

anti-apoptotic function in cancer cells. Furthermore, the upregulation of CK2 activity is connected with several diseases, including cancer, cardiac hypertrophy and ischaemic injury (Solimini *et al.*, 2007; Sarno and Pinna, 2008; Chua *et al.*, 2017; Franchin *et al.*, 2017). Thus, CK2 is considered as a promising drug target (Sarno and Pinna, 2008; Siddiqui-Jain *et al.*, 2012).

Several hundred CK2 substrates were identified that are involved in almost all physiological or biochemical processes. With the application of phosphoproteomics in combination with the characterization of kinase mutants, the number of reported putative CK2 substrates has increased further. In such studies, CK2 substrates were commonly defined by the identification of phosphorylation sites within the characteristic acidic motif (Reiland *et al.*, 2009). Recent data, however, suggested that this assignment overestimates the true number of CK2 targets because CK2 null mutants essentially lacking all CK2 activity showed phosphorylation activity on the typical CK2 consensus motifs and only one-third of the acidic phosphorylation sites were reduced in abundance (Franchin *et al.*, 2018). Several kinases were found to be upregulated in cells lacking CK2 activity, suggesting compensatory phosphorylation of crucial substrates by other kinases (Franchin *et al.*, 2018).

Instead of being integrated in signal cascades in a hierarchical order, CK2 was proposed as a lateral player that acts on entire signal cascades by enhancing or reducing the efficiency of signal propagation by other kinases. This is because CK2 is considered constitutively active. However, given the many targets of CK2 and the complex regulatory processes depending on CK2 activity, such as the assembly of the mitochondrial protein import machinery (Schmidt *et al.*, 2011), some regulation of CK2 activity likely exists. A potential key to this regulation lies in the subunit composition of the CK2 complex. CK2 may assemble into hetero-tetrameric complexes consisting of two catalytic α -, α' -subunits, and two regulatory β -subunits, or convey its catalytic activity alone by its catalytic α -subunits. Tetrameric complexes may occur in different forms such as $(CK2\alpha CK2\beta)_2$, $(CK2\alpha' CK2\beta)_2$ or $(CK2\alpha CK2\alpha')/(CK2\beta)_2$, and the latter can further aggregate into diverse multimeric complexes (Lolli *et al.*, 2017). Because the different CK2 complexes differ in activity, complex formation provides some regulatory access to CK2 activity with a certain degree of combinatorial possibilities.

Several CK2 isoforms exist in plants. Arabidopsis contains four CK2 alpha subunits: three of them nucleo-cytoplasmic and one chloroplast-localized (Salinas *et al.*, 2006; Mulekar and Huq, 2015). The chloroplast-localized enzyme has been termed plastid transcription kinase because of its activity on the plastid transcription system (Baginsky *et al.*, 1997). However, phosphoproteome analyses have uncovered several other putative CK2 targets, suggesting that it

may be involved in the regulation of different aspects of chloroplast functions (Reiland *et al.*, 2009; Bayer *et al.*, 2012). Plastid CK2 was furthermore implicated in the regulation of thermotolerance and the reduction of abscisic acid sensitivity and shown to be of general importance for multiple developmental processes in Arabidopsis, although the mechanistic basis for these functions is elusive (Wang *et al.*, 2014, 2016). Here, we set out to identify pCK2 targets in chloroplasts by phosphoproteomics and compared protein phosphorylation in illuminated and dark-adapted plastids. Plastid CK2 knockdown mutants have altered state transition kinetics, suggesting that pCK2 is involved in the regulation of photosynthetic acclimation. Metabolite profiling furthermore demonstrates a function of pCK2 in balancing metabolism to achieve optimal plant growth. In sum, our analysis provides an overview of pCK2 target proteins and reports previously unexpected functions for this ubiquitous kinase in plant-specific processes.

RESULTS

Isolation and phenotypic characterization of CK2 knockdown mutants

For a functional characterization of pCK2, we isolated homozygous plants from the GK615F11 mutant line that has a single T-DNA insertion in the first predicted exon (Figure 1a, Figure S1) (Wang *et al.*, 2016). This mutation results in a significantly decreased expression of pCK2 (At2g23070) but not of the neighbouring gene (At2g23080) (Figure 1b). We thus conclude that GK615F11 is a knockdown mutant that has a specific defect in the expression of plastid CK2, which is reduced to approximately 15% of wild-type levels in 2- and 4-week-old plants. We complemented the decrease in pCK2 expression with TAP-tagged pCK2 that was transformed into the *pck2* mutant background (Figure S1). The complementation line restored pCK2 transcripts to almost wild-type levels (Figure 1b). At the protein level, pCK2 is difficult to identify because of its low abundance (Schönberg *et al.*, 2014). Therefore, to increase the analytical sensitivity, we performed targeted analyses by multiple reaction monitoring (MRM). To this end, we spiked labelled peptides from pCK2 (Table S1) into the samples and searched for their native, unlabelled counterparts. This analysis identified unlabelled pCK2 peptides in wild-type and TAP-tagged pCK2 plants, but not in the knockdown lines (Figure S2, Table S1). This supports the view that pCK2 is absent from or of very low abundance in the knockdown lines, whereas it reaches detectable levels in wild-type and complementation lines.

Mutant plants grow slower on soil and on sucrose-containing media, although they are unaffected with respect to pigment accumulation or chloroplast development and differentiation (Wang *et al.*, 2016) (Figure 1c–e). Electron microscopic images of chloroplasts from wild-type and the

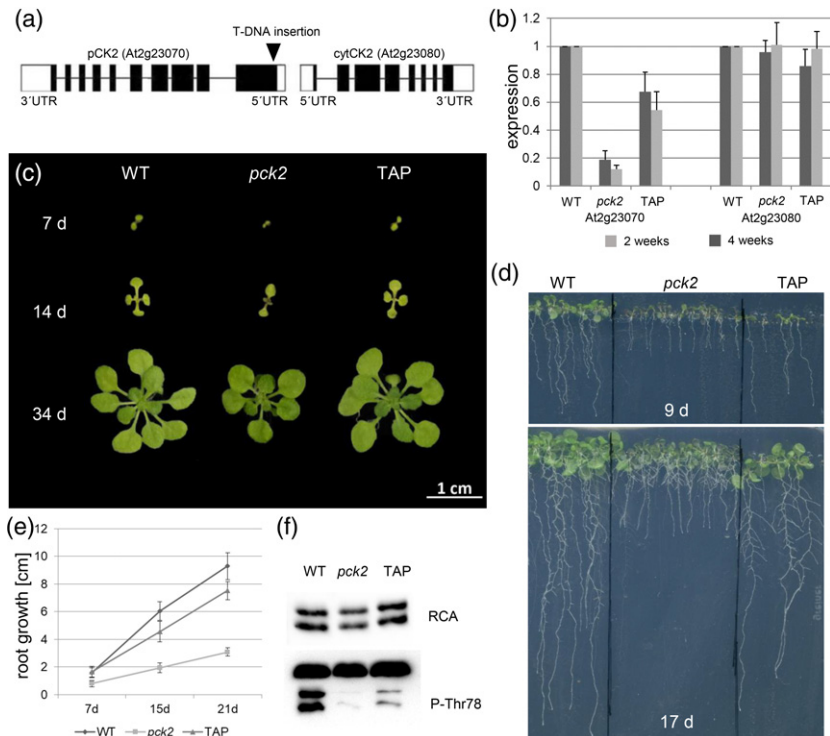


Figure 1. Characterization of the *pck2* knockdown mutant. (a) Gene model and position of the T-DNA insertion. (b) Expression analysis of the two neighbouring genes AT2g23070 and At2g23080 by quantitative RT-PCR, normalized on ubiquitin expression. (c, d) Examples for growth of the different plant lines on soil (c) and on plate (d). (e) Quantitative analysis of root growth. Error bars indicate the SD ($n = 25\text{--}38$). (f) Immunoblot showing the abundance of rubisco activase (RCA) and its phosphorylation state by Thr78-specific antibodies (Kim *et al.*, 2016).

pCK2 mutant revealed that chloroplast biogenesis is not affected by the mutation (Figure S3). The growth defect of *pck2* mutants was partially overcome in the TAP-tagged pCK2 complementation lines, as exemplified in Figure 1c–e, similar to that observed previously (Wang *et al.*, 2016). To determine whether diminished pCK2 activity is visible at the level of protein phosphorylation, we obtained antibodies against the established pCK2 phosphorylation site in RuBisCO activase (RCA) at threonine 78 (Kim *et al.*, 2016). The blot shows a significant reduction of RCA phosphorylation in the mutant that was partially restored in the complementation lines (Figure 1f, lower) (Kim *et al.*, 2016). Because RCA protein levels are not affected by the mutation (Figure 1f, upper), the data demonstrate that the phosphorylation state of RCA is reduced in the pCK2 mutant background, supporting diminished pCK2 activity in these plants.

Identification pCK2 targets by phosphoproteomics

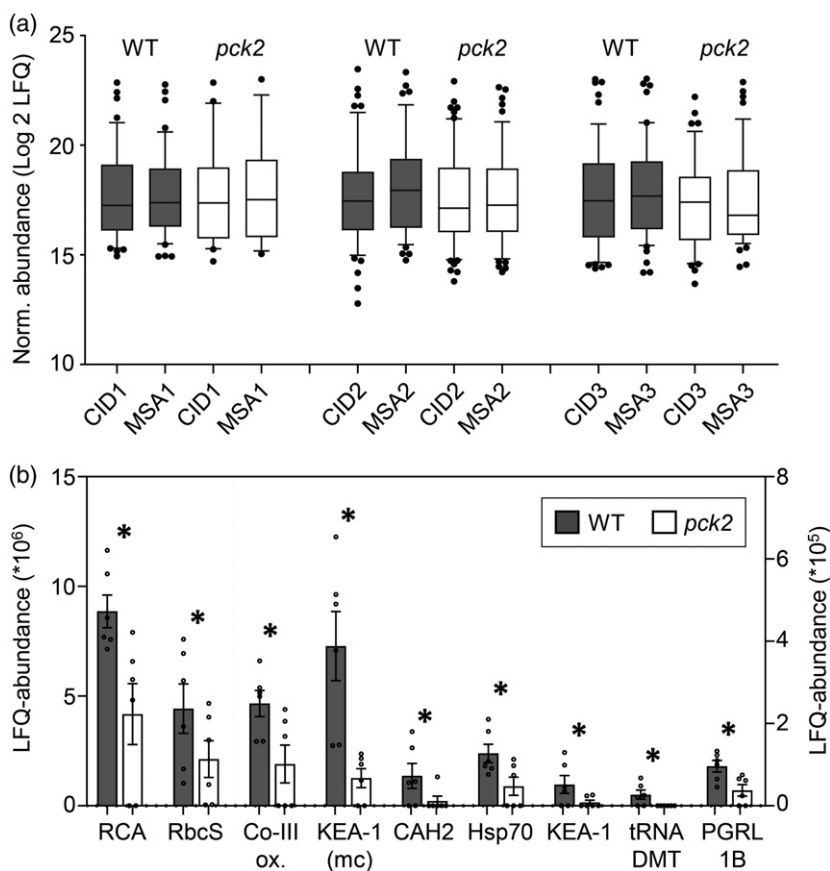
The depletion of pCK2 activity allowed us to identify putative pCK2 targets by their decreased phosphorylation state in the pCK2 knockdown mutants. Because the knockdown mutants potentially harbor residual pCK2 activity, robust phosphopeptide quantification was required to conclude on substrate connections. We therefore decided on a two-step workflow. First, we devised an untargeted survey analysis using wild-type and *pck2* plastid material. This analysis provided initial insights into which proteins might be targets of pCK2 by their decreased phosphorylation

state in the mutant. In the next step, we performed targeted analyses to increase the sensitivity of the analysis and to identify additional pCK2 substrates.

The survey scan was performed in three biological replicates using multistage activation (MSA) and collision-induced dissociation (CID) fragmentation methods, respectively (Schönberg *et al.*, 2017). Together, 296 plastid phosphoproteins, as annotated in SUBA (consensus localization) (Hooper *et al.*, 2017), were identified from wild-type and *pck2* knockdown plant material (Table S2). As expected, only a few chloroplast phosphoproteins were identified exclusively in wild-type and not in *pck2*. The ion current that is measured for a phosphopeptide can be used for relative quantification between different runs via label-free quantification (LFQ) approaches (Cox *et al.*, 2014; Tyanova *et al.*, 2016), provided that the data are normalized. We checked the normalization quality of MaxQuant LFQ-values for the wild-type and *pck2* samples and found them to be of sufficient quality for comparative quantitative analyses (Figure 2a). Based on these LFQ-values, a quantitative comparison identified eight proteins with a significantly higher phosphorylation state in wild-type compared to *pck2*. These comprise RCA, RbcS, coproporphyrinogen III oxidase, KEA-1 (with and without a missed cleavage site), PGRL1B, carbonic anhydrase 2, tRNA-dimethylallyltransferase and chloroplast HSP70 (Figure 2b, Table 1).

From the survey scan, we next selected those peptides that appeared to be likely pCK2 target peptides based on the reduction of their phosphorylation state in the *pck2*

Figure 2. Phosphopeptide quantification from light-grown plant chloroplasts by an untargeted approach. (a) Log₂-transformed label-free quantification distribution obtained from the identified phosphopeptides from the different measurements, namely three biological replicates (1–3), each acquired with two different scan types (multistage activation and collision-induced dissociation). (b) Phosphopeptides with significantly reduced abundance in *pck2* knockdown lines compared to wild-type (WT); an asterisk (*) indicates $P \leq 0.05$, t-test (two-sided). Data are the mean \pm SEM from three biological replicates with two scan types.



knockdown mutant versus wild-type and the phosphorylation of conspicuous acidic CK2 target motifs. Altogether, 38 peptides were selected for the target list, including the known pCK2 target peptide GLAYDTSDDQQDITR from RCA as a positive reference and the known Stn7/Stn8 target peptide LSGGDHIIHAGTVVGK from RBCL as a negative reference (Schönberg *et al.*, 2017, Table S3). Additionally, we added the peptide ALPTYTPESPGDATR from transketolase (TKL1) to the list. Recombinant pCK2 can phosphorylate TKL1 *in vitro*, although the phosphorylation site at Ser428 is phosphorylated in a Ca²⁺-dependent manner *in vivo* and thus is unlikely to be targeted by pCK2 (Rocha *et al.*, 2014). Based on the selected peptides, we devised an inclusion list to search for their specific *m/z* values in a range of 3 amu. We performed the experiment in three biological replicates with wild-type, *pck2* knockdown plants and the TAP-pCK2 complementation line from light-grown and dark-adapted plants (Figure S4).

The inclusion list identified 26 phosphopeptides in chloroplasts from light-grown plants (Table S4). We compared the abundance of phosphopeptides in knockdown plants and in the complementation lines with wild-type using the MaxQuant LFQ-values (Figure S4). Considering only those phosphopeptides that were identified in more

than one replicate, a set of 14 peptides showed a significant response to the mutation and/or the TAP-pCK2 complementation construct (Figure 3). For 12 other peptides we either could not obtain sufficiently reproducible information, or their phosphorylation state was not reduced in the mutant (Tables S2–S4, Figure S5). The two peptides GLAYDTSDDQQDITR in RCA (Figure 3) and LSGGDHIIHAGTVVGK in RBCL (Figure S5) showed an expected abundance distribution for target and non-target peptide. GLAYDTSDDQQDITR phosphorylation is significantly reduced in the mutants and partially restored by the TAP-pCK2 construct, similar to the immunoblotting results (Figures 1–3). The phosphorylation state of the non-target peptide LSGGDHIIHAGTVVGK from RBCL was not affected by the pCK2 mutation and the TAP-pCK2 construct, similar to the TKL1 phosphorylation site at Ser428 (Figure S5).

The LFQ-data show that Ser117/118/120 in K⁺-efflux antiporter 1 (KEA1), Ser133 in fructokinase-like 2 (FLN2), Ser741 in acetyl-CoA-carboxylase (CAC3), Thr48 in CP12, Ser837 in polyribonucleotide phosphorylase (PNPase), Ser81/Ser87 in phosphoglycerate kinase (PGK1), Ser56/Ser58 or Thr62 in outer envelope protein 6 (OEP6), Thr57 in fibrillin, Ser76/80 in the DEAD-box helicase RH3, Ser388 in a GPI-anchored protein, Thr76 in a ribosomal RNA small

Table 1 List of pCK2-responsive phosphorylation sites in light-grown and dark-adapted chloroplasts. Information is provided on the phosphopeptide and the most likely phospho-amino acid within the peptide. Phosphorylation sites were extracted from MaxQuant (Cox *et al.*, 2014; Tyanova *et al.*, 2016). In case of ambiguity, different alternative options are provided (note that all peptides listed carry only one phosphate). The peptides listed have a significantly different phosphorylation state between wild-type and the mutants. This could be either WT > pck2, TAP-pCK2 > pck2 or both ($P \leq 0.05$, *t*-test, two-sided). All information on the identifications is provided in Tables S2–S5

Untargeted analyses				
Accession	Name	Peptide sequence	Chloroplasts (light)	
AT2G39730	RCA	GLAYDTSDDQQDITR	Thr78	
AT1G67090	RbcS1A	EHGNSPGYYDGR	Ser113	
At4g11960	PGRL1B	ASTDQSGQVGGEEVDSK	Ser51/Thr52	
AT1G03475	Coproporphyrinogen- III-oxidase	DSDDVTPSSSSSSVR	Thr72	
AT5G14740	CAH2	VLAESSESAFEDQCGR	Ser193/194	
AT4G24280	cpHSP70	NQADSVVYQTEK	Ser612	
AT5G52960	tRNA-DMT	SSDAEEVSDTEDEWLK	Ser71	
AT1G01790	KEA1	IGESSESSDETEATDLKDAR	Ser117/118; Ser120	
Targeted analyses				
Accession	Name	Peptide sequence	Light-grown	Dark-adapted
AT1G69200	FLN2	AAAASSDVEEVKTEK	Ser133	Ser133
AT4G04020	FIB	ATDIDDEWQGDGVER	Thr57	–
AT2G46820	PSI-P	ATTEVGEAPATTEAETTELPEIVK	–	Thr65/66
AT3G63160	OEP6	DKSDSDDATVPPPSGA	Ser56; Ser58; Thr62	Ser56
AT5G63420	RNJ	ENSRDDDELADASDSEK	–	Ser805
AT2G47400	CP12	ATSEGEISEKVEK	Thr48	–
AT3G03710	PNPase	ALLPESETDKDSQK	Ser837	–
AT5G26742	RH3	SLGLSDHDEYDLGDNNNVEADDGEEAISK	Ser76; Ser80	–
AT2G38040	CAC3	ELAAEESDGSVKEDDDDDSSSESGK	Ser741	Ser741
AT1G01790	KEA1	IGESSESSDETEATDLKDAR	Ser117/118; Ser120	Ser117/118; Ser120
AT5G52960	tRNA-DMT	SSDAEEVSDTEDEWLK	Ser71	Ser71
AT5G14460	PSUFP	LYGSDSEIDENSSR	–	Ser132
AT3G49140	PPR-family	AGGDESEIDSSQDEK	–	Ser355
AT3G12780	PGK1	SVGDLTSADLK	Ser81; Ser87	Ser81; Ser87
AT5G23890	GPI anchored	SPVPESTDGSKDELNIYSQDELDDNR	Ser388	–
AT5G08540	rRNA MetJ	KNSSVEEETEEVEEDMPWIQEK	Thr76	–
AT4G20360	EF-Tu	SYTVTGVEMFQK	Thr332	–
AT5G14740	CAH2	VLAESSESAFEDQCGR	–	Ser193/194
At3g09050	8A-7O-S	SGDGTSDSDSDPPPKPEGDTR	–	Ser38, Ser43, Ser45
At4g02510	Toc159	VDGSESEETEEEMIFGSSEAAK	–	Ser630/632

subunit methyltransferase J (rRNA MetJ), Thr332 in elongation factor Tu (EF-Tu) and Ser71 in tRNA dimethylallyltransferase (tRNA DMT) are pCK2 targets because they can be identified in wild-type but not (or only significantly reduced) in the mutant, whereas the TAP-pCK2 partially restores their phosphorylation state (Figure 3, Table 1).

To increase the reproducibility and specificity in the identification of pCK2 targets, we searched for phosphorylation targets after a dark phase (end-of-night) (Reiland *et al.*, 2009). In dark-adapted plastids, Ser428 in TKL1 is also phosphorylated independently of pCK2 (Figure S5) thus supporting the light data and suggesting phosphorylation by a stroma-localized Ca^{2+} -dependent kinase (Rocha *et al.*, 2014). We find that Ser117/118/120 in KEA1, Ser133 in FLN2, Ser81/Ser87 in PGK1, Ser132 in pseudouridine synthase family protein (PSUFP), Ser71 in tRNA DMT,

Ser56 in OEP6, Ser741 in acetyl-CoA-carboxylase (CAC3), Ser193/194 in carbonic anhydrase (CAH2), Ser38/43/45 in 8-amino-7-oxononanoate synthase (8A-7O-S), Ser630/632 in Toc159 and Ser805 in ribonuclease J (RNJ) clearly show the characteristic features of pCK2 targets (Figure 3b, Table S5). The phosphorylation state of Thr65/66 in PSI-P (CURT1B) is significantly lower in the *pck2* knockdown plastids, although no restoration of phosphorylation levels was observed in the complementation lines (Figure 4). These data suggest that pCK2 is the kinase responsible for the previously observed light-independent basal phosphorylation level of PSI-P, whereas the lack of TAP-pCK2-mediated restoration of phosphorylation may be attributed to the inaccessibility of the phosphorylation site at the grana margins (Trotta *et al.*, 2019). The Ser355 phosphorylation site in a PPR-related protein showed pCK2 dependency in

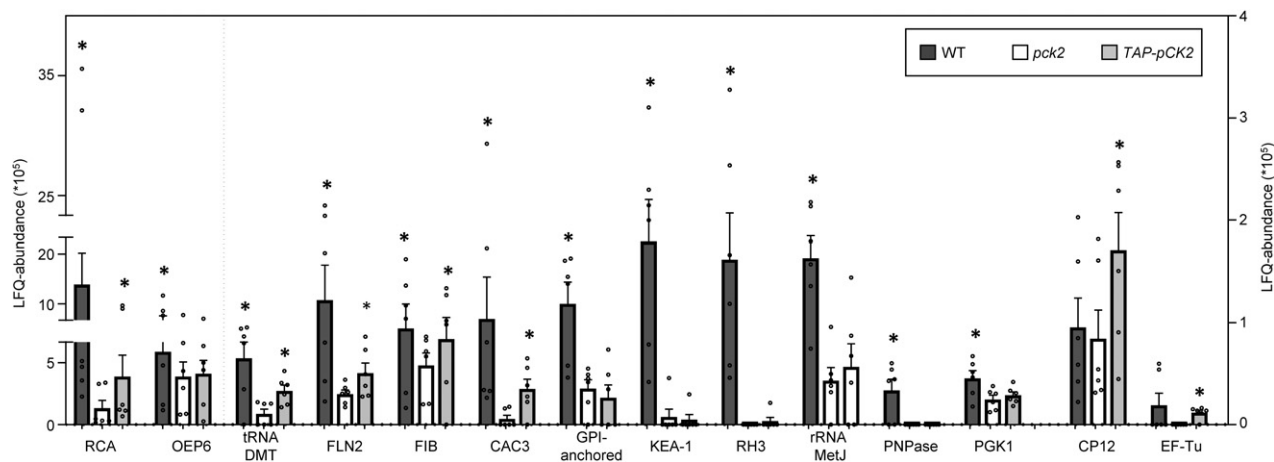


Figure 3. Phosphopeptide quantification from light-grown plant chloroplasts by a targeted approach. Provided are the label-free quantification (LFQ)-phosphopeptide abundance values determined by MaxQuant (Cox *et al.*, 2014) as the mean \pm SEM values from three biological replicates and two different scan types each. *P*-values were calculated from these LFQ-values by a *t*-test (two-sided). An asterisk (*) indicates $P \leq 0.05$ for the comparison between wild-type and *pck2*, as well as the comparison between *pck2* and TAP-pCK2. The dashed line separates the data points plotted on the left or right y-axis. Protein abbreviations represent the identifiers: RCA – AT2G39730; OEP6 – AT3G63160; tRNA DMT – AT5G52960; FLN2 – AT1G69200; FIB – AT4G04020; CAC3 – AT2G38040; GPI-anchored – AT5G23890; KEA-1 – AT1G01790; RH3 – AT5G26742; rRNA MetJ – AT5G08540; PNPase – AT3G03710; PGK1 – AT3G12780; CP12 – AT2G47400; EF-Tu – AT4G20360. All identified phosphopeptides are presented in Table 1.

dark- and light-adapted plastids, although only phosphorylation in the dark was significantly different between the mutants and wild-type (Figure 4 and Figure S5).

All data on putative pCK2 targets are summarized in Table 1. We performed quantitative proteomics by MSE (Helm *et al.*, 2014) with the wild-type, *pck2* and TAP-pCK2 plant material to assess the abundance of all putative pCK2 target proteins in the respective genotypes. An alignment around the phosphorylation site for the above mentioned pCK2 target peptides supports an over-representation of acidic amino acids in the +1 and +3 positions (Figure S6, Schönberg *et al.*, 2014). Except for PGRL1B, OEP6 and Toc159, all proteins are equally abundant in wild-type and *pck2* knockdown plants; thus, it is their phosphorylation state and not overall protein abundance that is affected by the mutation in *pck2* (Figure S7). Together, both datasets support the notion that the identified proteins are direct targets of pCK2.

The *pck2* mutants show altered state transition kinetics and significant remodelling of metabolism

We identified several thylakoid membrane proteins as putative pCK2 targets, suggesting pCK2-mediated regulatory connections between different chloroplast functions. Because photosynthetic acclimation is an important target for post-translational regulation (Rochaix, 2014; Koskela, *et al.*, 2018), we assessed the functioning of state transitions in the mutant compared to wild-type by chlorophyll fluorescence change measurements in response to incident light quality shifts. Both wild-type and *pck2* mutants displayed a functional state transition. However, in the mutant, state 1-to-state 2 transitions were found to run

considerably slower than in wild-type because their half-life decay of fluorescence was significantly delayed (Figure 5 and Figures S8 and S9). The degree of LHCII phosphorylation (typically responsible for the state transition) in both mutants and wild-type as determined by P-Thr antibodies was comparable with a low phosphorylation state under PSI-light and a high one under PSII-light (Figure 5). This result led us to conclude that the redox-regulated phosphorylation of the major LHCII by the Stn7 kinase is fully functional in the mutant and therefore is unlikely to be involved in the observed deceleration of the state 1-to-state 2 transition. It is thus possible that the pCK2-dependent phosphorylation of, for example, PSI-P at Thr65/66 reported here may be involved in the deceleration of state transitions, although detailed functional characterizations must follow.

Earlier studies reported a reorganization of chloroplast metabolism in response to differences in the plastoquinone redox state (Bräutigam *et al.*, 2009). Because the latter is interlinked with state transitions, we assessed the metabolic state of wild-type and *pck2* plants by metabolite profiling on leaves of wild-type and *pck2* plants with a particular focus on carbohydrate, organic acid and amino acid metabolism. Polar metabolites were extracted from 2-, 4-, 5- and 6-week-old plants and quantified by GC-MS. In total, 49 metabolites were quantified, including 18 amino acids, 11 organic acids, 10 sugars and sugar alcohols, and 10 miscellaneous compounds. Figure 5 shows the metabolic changes in the mutant with respect to the wild-type. We observed alterations in the amino acid composition (e.g. glutamine and glycine showed increases of up to 73-fold and 65-fold in the mutant compared to wild-type). On the

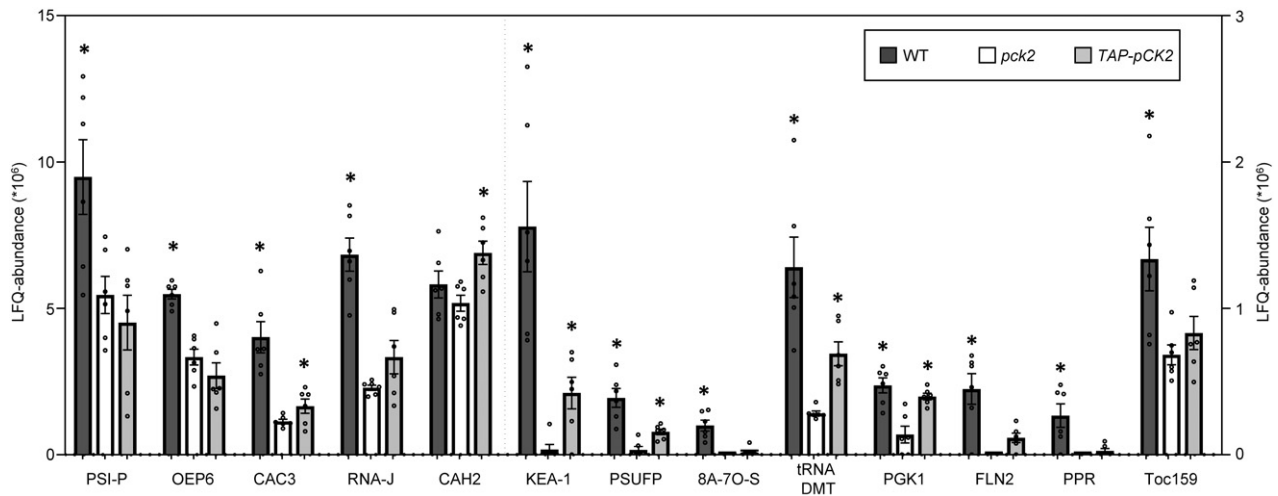


Figure 4. Phosphopeptide quantification from dark-adapted plant chloroplasts by a targeted approach. Provided are the label-free quantification (LFQ)-phosphopeptide abundance values determined by MaxQuant (Cox *et al.*, 2014) as the mean \pm SEM from three biological replicates and two different scan types each. *P*-values were calculated from these LFQ-values by a *t*-test (two-sided). An asterisk (*) indicates $P \leq 0.05$ for the comparison between WT and *pck2*, as well as the comparison between *pck2* and TAP-pCK2. The dashed line separates the data points plotted on the left or right y-axis. Protein abbreviations represent the identifiers: PSI-P – AT2G46820; OEP6 – AT3G63160; CAC3 – AT2G38040; RNA-J – AT5G63420; CAH2 – AT5G14740; KEA-1 – AT1G01790; PSUFP – AT5G14460; 8A-7O-S – AT3g09050; tRNA DMT – AT5G52960; PGK1 – AT3G12780; FLN2 – AT1G69200; PPR – AT3G49140; Toc159 – At4g02510. All identified phosphopeptides are presented in Table 1.

other hand, some amino acids (e.g. isoleucine, lysine, tryptophan and tyrosine) were significantly decreased in the mutant. Most organic acids, sugars and sugar alcohols are decreased in *pck2* plants (Figure 6 and Table S6). Aspartic acids, succinic acid and threonic acid were most significantly different in this class of metabolites. The data suggest that mutant plants have a significantly altered metabolism, supporting pleiotropic activity of pCK2 and an important function in balancing metabolic activity for optimal performance.

DISCUSSION

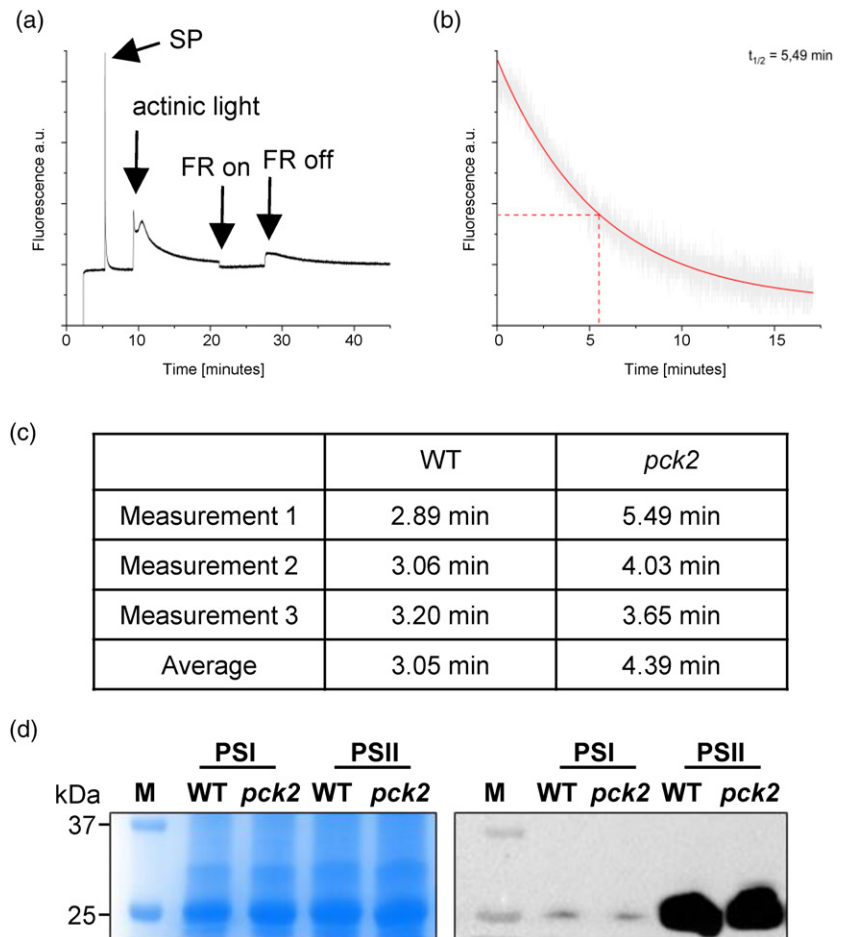
We report here a comparative analysis of protein phosphorylation states in a *pck2* knockdown mutant compared to wild-type by targeted and non-targeted phosphoproteomics. The *pck2* mutant GK615F11 used in the present study carries a single T-DNA insertion in the first exon (Figure S1), resulting in a severe growth phenotype with significantly shortened primary roots (Figure 1). This phenotype has been observed previously by Wang *et al.* (2016) but stands in contrast to the mutant GABI400A04 that shows no growth phenotype with a T-DNA insertion in the fifth exon of pCK2 (Kim *et al.*, 2016). It is difficult to align the different phenotypes, although it is possible that the latter line produces limited amounts of functional enzyme, thus resulting in the mild growth phenotype. The successful complementation of the phenotype reported in the present study and by Wang *et al.* (2016) clearly shows that a defect in pCK2 is responsible for the growth and developmental defects, suggesting that casein kinase activity in plastids is important to ensure optimal plant

performance. Thus, the identification of its *in vivo* targets is important to understand how the plastid phosphorylation network balances plant metabolism to accomplish proficient plant growth.

Based on the reduction of phosphorylation state in the kinase mutant, we indirectly infer a kinase substrate relationship for several proteins with pCK2. We are aware that this inference is indirect and neglects the possibility that effects such as developmental state, adaptations in the proteome to the kinase mutants and the resulting inaccessibility of otherwise used phosphorylation sites may lead to false target protein assignments. However, by carefully evaluating target protein abundance between wild-type and kinase mutants (Figure S7), by checking the characteristics of the phosphorylation sites used by pCK2 (Figure S6) and by using a TAP-pCK2 complementation line that partially restores the phosphorylation state of target proteins in the mutant background, we reduced false assignments and increased the significance of our data (Figures 1–4). Our analysis shows that the kinase introduced with the complementation construct restores growth parameters, as well as the phosphorylation state of many target proteins. Interestingly, not all proteins are equally well accepted as substrate for the complementing kinase, suggesting regulatory processes *in vivo* (e.g. on the accessibility of phosphorylation sites). This information is important for *in vivo* strategies that are designed to operate with overexpressed kinases.

CK2 mutants for comparative phosphoproteomics were used before and our observations are in line with some of the peculiarities of such previous studies. For example,

Figure 5. Analysis of state transitions in wild-type and the *pck2* mutant. (a, b) Kinetic fluorescence measurements and (c) half-life values for the transition from state 1 to state 2. (d) Coomassie stain of isolated thylakoids and immunoblotting with P-threonine-specific antibodies with wild-type and *pck2* mutant plant material after adaptation of the plants to photosystem (PSI) or PSII light, as indicated (Experimental procedures).



phosphorylation of typical CK2 consensus phosphorylation motifs was frequently observed in CK2 null mutants (Rusin *et al.*, 2017; Franchin *et al.*, 2018). This was interpreted as compensatory phosphorylation by other protein kinases. In our data, we find examples for this unexpected situation, most strikingly for the ALB3 phosphorylation site at Ser424 that has been identified on peptide chips and in an *in vitro* phosphorylation assay as pCK2 substrate (Schönberg *et al.*, 2014). Surprisingly, the phosphorylation state of the ALB3 phosphopeptide is significantly increased in the *pck2* knockdown lines (Figure S4). A possible explanation is the compensatory phosphorylation of pCK2 target proteins by other kinases. On the other hand, CK2 depletion has a reported effect on non-target sites in cell cultures, as exemplified for the serine/proline and threonine/proline phosphorylation motifs (St-Denis *et al.*, 2015; Rusin *et al.*, 2017; Franchin *et al.*, 2018). The survey phosphoproteome analysis performed here also identified two more proteins with a higher phosphorylation state in the mutant: the beta subunit of ATPase (ATCG00480, *P*-value 0.008) and LHCA1 (AT3G61470, *P*-value 0.05) (Table S2).

The set of pCK2 target proteins in chloroplasts supports its pleiotropic nature and comprises proteins with a diverse set of biological functions. The majority of the putative pCK2 targets identified here are independent of the Stn7/Stn8 kinases at the thylakoid membrane, as indicated by their phosphorylation in the *stn7/stn8* double mutant background (Schönberg *et al.*, 2017). Consistently, some, but not all, pCK2 targets are phosphorylated in a light-independent manner. We failed to detect known pCK2 targets such as pTAC10 (Schönberg *et al.*, 2014; Yu *et al.*, 2018) under our growth conditions, suggesting additional regulatory processes operating on pCK2 targets. Although CK2 is generally considered constitutively active (Franchin *et al.*, 2017), an effect of reduced GSH was reported for plastid CK2 (Baginsky *et al.*, 1999; Turkeri *et al.*, 2012). In line with a potential redox regulation, we observed slowed state transition kinetics and altered primary metabolism in the *pck2* mutant plants (Figures 4 and 5). The effect on photosynthetic acclimation processes could be mediated by KEA1 or PSI-P (CURT1B) phosphorylation, where PSI-P determines the accessibility of phosphorylation sites in the major antenna complexes (Figure 4). Further experiments

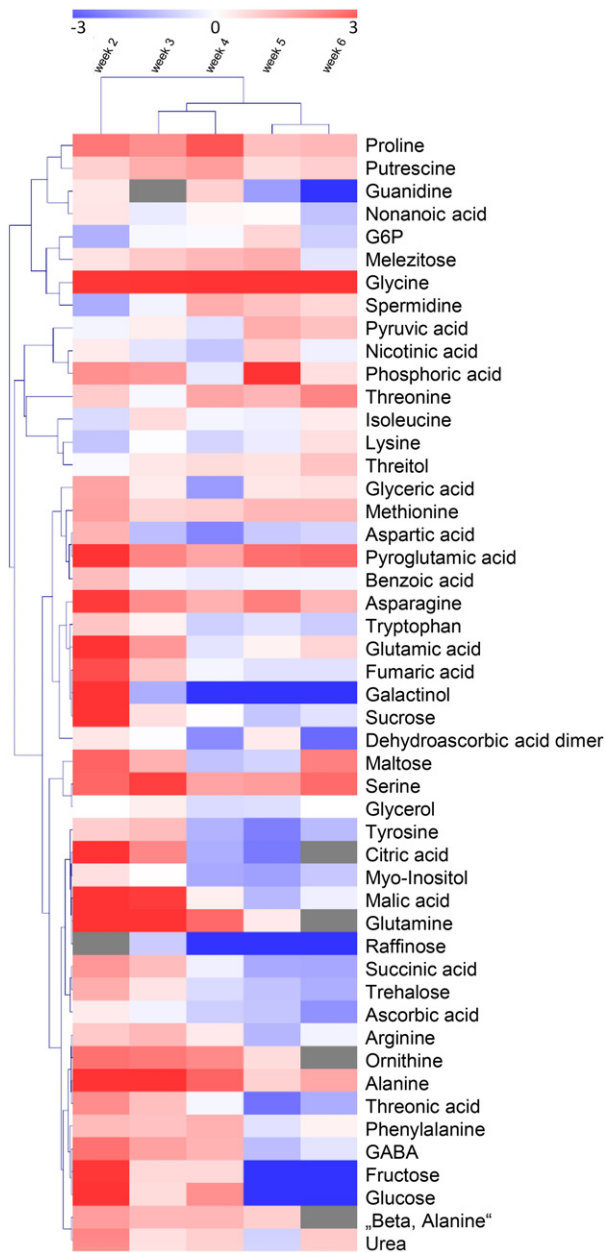


Figure 6. Hierarchical clustering of metabolite profiling data. Metabolite profiling data obtained by GC-MS of *pck2* mutants and wild-type with 2-, 3-, 4-, 5- and 6-week-old plants expressed as the log₂-ratio between mutant and wild-type. The ratio is presented as a heat-map (for colour coding, see the uppermost panel).

are necessary to unravel the functional connections in the pCK2 triggered chloroplast phosphorylation network.

The metabolic profiling data, obtained from approximately 50 derivatized polar metabolites by GC-MS, indicate massive changes in amino acids levels between *pck2* and wild-type plants. In particular, two amino acids, glycine and glutamine, showed a dramatic change in abundance.

This could be a consequence of the phosphorylation of CP12, for example. CP12 is found almost universally among photosynthetic organisms where it plays a key role in the regulation of the Calvin cycle by forming a ternary complex with glyceraldehyde 3-phosphate dehydrogenase and phosphoribulokinase (Howard *et al.*, 2011; Stanley *et al.*, 2013). Its phosphorylation at Thr48 is light-dependent, which is in line with its function in the Calvin cycle. Although amino acid biosynthetic enzymes were not identified as direct targets of pCK2, it is not surprising that their abundance is dynamically altered because the vast majority of them are synthesized in the plastid. This is supported by the fact that the abundances of most amino acids are changed when the ATP supply of this organelle is diminished (Carrari *et al.*, 2005). A potentially important observation for the regulation of metabolism is the phosphorylation of the alpha subunit of acetyl-CoA-carboxylase (AT2G38040). The phosphorylation site at Ser741 is clearly pCK2-dependent, as indicated by its significantly decreased abundance in the *pck2* knockdown plants and its restoration by the TAP-pCK2 construct, both in the light and after a dark phase (Figures 3 and 4). At present, the influence of this phosphorylation site on lipid or fatty acid biosynthesis remains unclear because only polar metabolites were covered by our metabolic profiling analysis. In general, it is difficult to directly connect the metabolic phenotype with the targets of pCK2 as a result of its pleiotropy. For example, the differences in organic acid concentration suggest cross-talk with mitochondrial function in energy metabolism. Whether this is an indirect effect or whether pCK2 is dually targeted to chloroplast and mitochondria remains unclear at present.

With the set of pCK2 target proteins identified here, we provide further details on the chloroplast phosphorylation network. We find connections between the stroma-localized pCK2 and the thylakoid-associated kinases Stn7/Stn8 with respect to the regulation of different chloroplast functions, such as photosynthetic acclimation, gene expression and metabolism (Schönberg *et al.*, 2017). Surprisingly, depletion of the pleiotropic pCK2 has only a minor effect on chloroplast differentiation and development, whereas it significantly affects the metabolic status of the chloroplast and, consequently, plant growth. Thus, pCK2 may function as a balancer between different metabolic activities to reach an optimal output. How this is achieved and how this is regulated remain topics for further research.

EXPERIMENTAL PROCEDURES

Plant growth and chloroplast isolation

Arabidopsis thaliana plants Col-0 (wt) and mutant GK615F11 were grown on a soil/vermiculite mixture (4:1) in a controlled environment chamber under short-day conditions (8:16 h light/dark photoperiod, 150 $\mu\text{mol m}^{-2} \text{sec}^{-1}$).

GK615F11 is a single insertion line, as suggested by segregation analysis resulting in $20 \pm 4.4\%$ sensitivity to sulfadiazine ($30 \mu\text{g ml}^{-1}$ in 0.5 MS). Resistant plants were screened for homozygosity (Figure S1) and homozygous plants were used for further characterization (Figure S1, Table S7). 'Line 10' (Figure S1b) was used for complementation analysis. To this end, we transformed plants with pEG205-TAP-CK2 + TP (Earley *et al.*, 2006) via *Agrobacterium tumefaciens*, selected for BASTA resistant lines and genotyped the resulting plants by PCR (Figure S1c, Table S7). The construct comprises pCK2 with an N-terminal transit peptide and a C-terminal TAP fusion. A single complementation line was used for further analyses. Plants were harvested after 14 or 28 days, as indicated. Chloroplasts were isolated in accordance with established protocols (Fitzpatrick and Keegstra, 2001).

Photosynthetic light quality acclimation and state transition measurements

For testing the light quality acclimation abilities of pCK2 mutants, *A. thaliana* Col 0 and pCK2 mutant plants were grown in parallel for 13 days under white light (days 1–7: long-day condition, 16:8 h light/dark photoperiod, approximately $50 \mu\text{mol m}^{-2} \text{sec}^{-1}$; days 8–13: continuous light, approximately $35 \mu\text{mol m}^{-2} \text{sec}^{-1}$) followed by 3 days of either continuous PSII- or PSI-lights. The specificities of PSII- and PSI-light sources were essentially as described previously (Wagner *et al.*, 2008; Dietzel *et al.*, 2011). State transitions were measured on plants directly in their growth trays via non-invasive chlorophyll fluorescence measurements. The courses of state transition-associated fluorescence changes were determined in accordance with standard protocols using a PAM101 fluorometer (Walz, Effeltrich, Germany) (Lunde *et al.*, 2000; Damkjaer *et al.*, 2009). Determination of kinetics and calculations of half-lives of state 1-to-state 2 transitions were performed as described previously (Dietzel *et al.*, 2011). Detection of the phosphorylation state of light-harvesting complex proteins after acclimation to either PSII- or PSI-light was achieved by immunoblotting and western blotting analysis. Plants from the same batch as used for chlorophyll fluorescence were harvested under growth light conditions, and then immediately frozen into liquid nitrogen and ground to a fine powder. Total protein extracts were generated in accordance with published protocols and samples were separated by denaturing SDS-PAGE followed by western blotting. Phosphorylated proteins were detected with a commercially available polyclonal primary rabbit-anti-phosphothreonine antibody as described previously (Dietzel *et al.*, 2011).

Chloroplast protein preparation

Isolated chloroplasts were resuspended at 4°C in a buffer containing 50 mM TRIS/HCl, pH 7.6, 0.1% protease inhibitor

cocktail (P9599; Sigma, St Louis, MO, USA) and $0.1\times$ Phos-STOPTM (Roche, Basel, Switzerland). Ice-cold acetone ($9\times$ volume) was added to the chloroplast suspension. The mixture was incubated overnight at -20°C and centrifuged at $20\,000\text{ g}$ for 5 min at 4°C . The pellet was washed twice with ice cold 90% acetone and dried at room temperature.

Tryptic digest and phosphopeptide enrichment

In total, 1 mg of the acetone precipitated chloroplast proteins was digested with trypsin (Promega, Madison, WI, USA). Phosphopeptides were subsequently enriched with a spin-tip filled with TiO_2 as described previously (Schönberg *et al.*, 2017).

Protein extraction and immunoblotting

SDS-PAGE was conducted as described previously (Wessel and Flugge, 1984). The chloroplasts were resuspended in SDS sample buffer [50 mM Tris-HCl pH 6.8, 2% (w/v) SDS, 10% (v/v) glycerol, 0.1 mM DTT, 0.04% bromophenol blue], heated at 80°C for 5 min and centrifuged for 5 min at $20\,000\text{ g}$. The supernatant equivalent to $5 \mu\text{g}$ of chlorophyll was loaded onto a 12% polyacrylamide SDS gel. Subsequent to electrophoresis the proteins were transferred to polyvinylidene difluoride membranes via semi-dry blotting. Immunodetection was conducted by chemiluminescence using a Fusion Fx7 illumination system (Vilber, Marne-la-Vallée, France). Primary antibodies against RCA P-Thr78 were generously provided by Kim *et al.* (2016).

Protein identification and quantification using the Synapt G2-S mass spectrometer

Tryptically digested samples from protein extracts obtained from isolated chloroplasts were dissolved in 2% (v/v) acetonitrile and 0.1% (v/v) formic acid and injected into an ACQUITY UPLC System connected to a Synapt G2-S mass spectrometer (Waters Corp., Eschborn, Germany). Nano-LC separation (140 min gradient) and high-definition (HD)-MSE data acquisition was conducted as described previously (Helm *et al.*, 2014). MS acquisition was set from 50–2000 Da. Data analysis was carried out via the ProteinLynx Global Server (PLGS 3.0.1, Apex3D algorithm version 2.128.5.0, 64 bit; Waters Corp.) with automated determination of chromatographic peak width as well as MS-time of flight resolution. Lock mass value for charge state 2 was defined as 785.8426 Da/e and the lock mass window was set to 0.25 Da. Low/high energy threshold was set to 180/15 counts, respectively. Elution start time was at 5 min, intensity threshold was set to 750 counts. For the databank search query (PLGS workflow): peptide and fragment tolerances were set to automatic, with two fragment ion matches per peptide, five fragment ions for protein identification and two peptides per protein. Maximum protein mass was set to 250 kDa. Primary digest reagent was trypsin with one missed cleavage allowed. According to the

digestion protocol fixed (carbamidomethyl on Cys) and variable (oxidation on Met) modifications were set. The false discovery rate (FDR) was set to 4% at the protein level. MSE data were searched against the modified *A. thaliana* database (TAIR10; <ftp://ftp.arabidopsis.org>) containing common contaminants (<ftp://ftp.thegpm.org/fasta/cRAP/crap.fasta>) and rabbit glycogen phosphorylase B (P00489) was used as an internal quantification standard (Helm *et al.*, 2014).

To search for pCK2 in plant extracts, we performed targeted assays using isotopically labelled peptides. To this end, we spiked 12.5 fmol labeled proteotypic peptides of pCK2 into wild-type, *pck2* knockdown and *pck2* knockdown/TAP pCK2 extracts. We searched for the labeled peptides by a modified MRM method on a Synapt G2-S (Waters Corp.) with MassLynx 4.1 SCN916 (Waters Corp.). In brief, the HD-MRM scan time was set to 0.15 sec and the orthogonal acceleration pusher and the ion mobility separation were synchronized (wideband enhancement). Furthermore, the LM resolution of the quadrupole was adjusted from 4.7 to 7.0 to narrow the isolation window of the quadrupole. For the SIL peptides, a database containing only these peptides was created and the database search query was adjusted, such that only one peptide was necessary for identification. As a result of their isotope label, SILAC modification on lysine (U-¹³C₆; U-¹⁵N₂) and arginine (U-¹³C₆; U-¹⁵N₄) was set as the fixed modification.

Protein identification using an 'Orbitrap Velos Pro' mass spectrometer

Peptides were injected into an EASY-nLCII liquid chromatography system (Thermo Fisher Scientific, Waltham, MA, USA) and separated using C18 reverse phase chemistry employing a pre-column (EASY column SC001, length 2 cm, inner diameter 100 µm, particle size 5 µm) in line with an EASY column SC200 (length 10 cm, inner diameter 75 µm, particle size 3 µm) (both from Thermo Fisher Scientific). Peptides were eluted into a Nanospray Flex ion source (Thermo Fisher Scientific) with a 180 min gradient increasing from 5 to 40% acetonitrile in ddH₂O with a flow rate of 300 nl min⁻¹ and electrosprayed into an Orbitrap Velos Pro mass spectrometer (Thermo Fisher Scientific). The source voltage was set to 1.9 kV and the S Lens RF level was 50%. The delta multipole offset was -7.00. The phospho-peptide fraction was measured with a data-dependent acquisition scan strategy with one MS full scan with a resolution of 30 000 preceding up to 20 MS/MS fragment ion scans. The repeat count was set to 1, the repeat duration to 30 sec, the exclusion duration to 40 sec and the exclusion width to 10 p.p.m. of the precursor *m/z*. Full scan MS spectra were internally calibrated on the fly with the ambient ion *m/z* 445.120024. The AGC target value was set to 1 × 10⁶ and the maximum injection time was 500 ms in the Orbitrap. The parameters were set to

1 × 10⁴ and 200 ms in the linear quadrupole ion trap with an isolation width of 2 Da for precursor isolation and MS/MS scanning. Additionally, measurements were performed with the inclusion list to specifically target certain phosphorylated peptides. Two fragmentation regimes were employed for MS/MS phosphopeptide sequencing. Conventional CID and CID with MSA were performed to further fragment the ion peaks resulting from neutral loss of the phosphate moiety by dissociation of the high energy phosphate bond to generate MS/MS spectra with more intense b- and y-fragment ion series rich in peptide sequence information.

MS raw files were analyzed using MaxQuant, version 1.6.10.43, for phosphopeptide assignment (Tyanova *et al.*, 2016). The search engine was used with default settings, including PSM, peptide and protein FDR set at 1% and match between runs enabled. The *A. thaliana* database (Araport11; <https://www.arabidopsis.org>) with contaminants included was used as the analytical basis. Precursor mass tolerance was set to 20 p.p.m. and the fragment ion tolerance was 0.5 Da. Carbamidomethylation of cysteines was set as the fixed modification and oxidation of methionine, acetylation of protein N-termini, pyroglutamate formation and phosphorylation of serine and threonine as variable modification, with two missed cleavages allowed. For quantification by the MaxLFQ algorithm (Cox *et al.*, 2014) a minimum ratio count of two unique or razor peptides was required. The MS data were uploaded to the ProteomeXchange consortium at PRIDE (<https://www.ebi.ac.uk/pride>) and are available under accession PXD014930.

GC-MS

Extraction and analysis by GC-MS was performed using the same equipment set-up and the exact same protocol as that described by Lisec *et al.* (2006). Briefly, frozen ground material was homogenized in 700 µl of methanol at 70°C for 15 min and then 375 µl of chloroform followed by 750 µl of water were added. The polar fraction was dried under vacuum, and the residue was derivatized for 120 min at 37°C (in 40 µl of 30 mg ml⁻¹ methoxyamine hydrochloride in pyridine) followed by a 30 min of treatment at 37°C with 70 µl of *N*-trimethylsilyl-*N*-methyl trifluoroacetamide. An autosampler MultiPurpose system (Gerstel, Mülheim, Germany) was used to inject the samples into a chromatograph coupled to a time-of-flight MS (GC-MS) system (Pegasus HT TOF-MS; Leco, St Joseph, MI, USA). Helium was used as carrier gas at a constant flow rate of 2 ml sec⁻¹ and GC was performed on a 30 m DB-35 column (Agilent, Santa Clara, CA, USA). The injection temperature was 230°C and the transfer line and ion source were set to 250°C. The initial temperature of the oven (85°C) increased at a rate of 15°C min⁻¹ up to a final temperature of 360°C. After a solvent delay of 180 sec,

mass spectra were recorded at 20 scans sec⁻¹ with a scanning range of *m/z* 70–600. Chromatograms and mass spectra were evaluated using Chroma TOF, version 4.5 (Leco) and TagFinder, version 4.2 (Luedemann *et al.*, 2008). Heat maps were created with MeV software (<http://www.tm4.org/mev.html>), using the log₂ of the fold changes to average all of the data across all tissues.

ACKNOWLEDGEMENTS

We are grateful for financial support from the DFG, grant number 'BA 1902/2-2' and the European Regional Development Fund of the European Commission grant W21004490 via Land Sachsen-Anhalt to SB. SB gratefully acknowledges DFG support for the acquisition of a Synapt G2-S mass spectrometer (INST 271/283-1 FUGG). We thank Monika Grycko for her help in the state transition experiments and Jessica Fostvedt for mutant characterization. Open access funding enabled and organized by Projekt DEAL.

CONFLICT OF INTEREST

The authors declare no conflict of interest.

AUTHOR CONTRIBUTIONS

AR, BA and SB designed the research; AR, JG, EB, BA, SH, SA, ARF, DT, WH, GH, TP and SB performed the research and analyzed the data; AR, BA and SB wrote the paper.

DATA AVAILABILITY STATEMENT

All MS data were uploaded to PRIDE (<https://www.ebi.ac.uk/pride>) and are accessible under the identifier PXD014930. All other data are available in the text and in the supplement.

SUPPORTING INFORMATION

Additional Supporting Information may be found in the online version of this article.

Figure S1. Characterization of *pck2* mutants and generation of complementation construct.

Figure S2. Example for the MRM-based identification of the pCK2 peptide IELDPNLTSLVGR in the different plant lines.

Figure S3. Electron microscopic images of chloroplasts from wild-type and *pck2* knockdown lines.

Figure S4. Normalization of the quantitative read-out for the identified phosphopeptides.

Figure S5. Quantitative depiction of non-target phosphopeptides in wild-type, *pck2* and TAP-pCK2 lines.

Figure S6. Alignment of pCK2-target peptides by WebLogo.

Figure S7. Quantification of pCK2 target proteins by MSE and the Hi3 method.

Figure S8. Kinetic fluorescence measurements with wild-type plants.

Figure S9. Kinetic fluorescence measurements with *pck2* plants.

Table S1. Heavy peptides used for MRM analyses along with expected and detected transitions.

Table S2. Results of untargeted phosphoproteome surveys.

Table S3. Target list for phosphopeptide detection.

Table S4. Results from targeted surveys obtained with light-grown plants.

Table S5. Results from targeted surveys obtained with dark-adapted plants.

Table S6. Quantitative results obtained from metabolite profiling data.

Table S7. List of primers used.

REFERENCES

- Baginsky, S., Tiller, K. and Link, G. (1997) Transcription factor phosphorylation by a protein kinase associated with chloroplast RNA polymerase from mustard (*Sinapis alba*). *Plant Mol. Biol.* **34**, 181–189.
- Baginsky, S., Tiller, K., Pfannschmidt, T. and Link, G. (1999) PTK, the chloroplast RNA polymerase-associated protein kinase from mustard (*Sinapis alba*), mediates redox control of plastid in vitro transcription. *Plant Mol. Biol.* **39**, 1013–1023.
- Basnet, H., Su, X.B., Tan, Y., Meisenhelder, J., Merkurjev, D., Ohgi, K.A., Hunter, T., Pillus, L. and Rosenfeld, M.G. (2014) Tyrosine phosphorylation of histone H2A by CK2 regulates transcriptional elongation. *Nature*, **516**, 267–271.
- Bayer, R.G., Stael, S., Rocha, A.G., Mair, A., Vothknecht, U.C. and Teige, M. (2012) Chloroplast-localized protein kinases: a step forward towards a complete inventory. *J. Exp. Bot.* **63**, 1713–1723.
- Bräutigam, K., Dietzel, L., Kleine, T. *et al.* (2009) Dynamic plastid redox signals integrate gene expression and metabolism to induce distinct metabolic states in photosynthetic acclimation in Arabidopsis. *Plant Cell*, **21**, 2715–2732.
- Carrari, F., Coll-Garcia, D., Schauer, N., Lytvchenko, A., Palacios-Rojas, N., Balbo, I., Rosso, M. and Fernie, A.R. (2005) Deficiency of a plastidial adenylate kinase in Arabidopsis results in elevated photosynthetic amino acid biosynthesis and enhanced growth. *Plant Physiol.* **137**, 70–82.
- Chua, M.M., Ortega, C.E., Sheikh, A., Lee, M., Abdul-Rassoul, H., Hartshorn, K.L. and Dominguez, I. (2017) CK2 in cancer: cellular and biochemical mechanisms and potential therapeutic target. *Pharmaceuticals (Basel)*, **10**, 18.
- Cox, J., Hein, M.Y., Luber, C.A., Paron, I., Nagaraj, N. and Mann, M. (2014) Accurate proteome-wide label-free quantification by delayed normalization and maximal peptide ratio extraction, termed MaxLFQ. *Mol. Cell Proteomics*, **13**, 2513–2526.
- Damkjaer, J.T., Kereiche, S., Johnson, M.P., Kovacs, L., Kiss, A.Z., Boekema, E.J., Ruban, A.V., Horton, P. and Jansson, S. (2009) The photosystem II light-harvesting protein Lhcb3 affects the macrostructure of photosystem II and the rate of state transitions in Arabidopsis. *Plant Cell*, **21**, 3245–3256.
- Dietzel, L., Bräutigam, K., Steiner, S., Schöffler, K., Lepetit, B., Grimm, B., Schöttler, M.A. and Pfannschmidt, T. (2011) Photosystem II super-complex re-modeling serves as entry mechanisms for state transitions in Arabidopsis. *Plant Cell*, **23**, 2964–2977.
- Earley, K.W., Haag, J.R., Pontes, O., Oppen, K., Juehne, T., Song, K. and Pikaard, C.S. (2006) Gateway-compatible vectors for plant functional genomics and proteomics. *Plant J.* **45**, 616–629.
- Fitzpatrick, L.M. and Keegstra, K. (2001) A method for isolating a high yield of Arabidopsis chloroplasts capable of efficient import of precursor proteins. *Plant J.* **27**, 59–65.
- Franchin, C., Borgo, C., Cesaro, L., Zaramella, S., Vilardeil, J., Salvi, M., Arrigoni, G. and Pinna, L.A. (2018) Re-evaluation of protein kinase CK2 pleiotropy: new insights provided by a phosphoproteomics analysis of CK2 knockout cells. *Cell. Mol. Life Sci.* **75**, 2011–2026.
- Franchin, C., Borgo, C., Zaramella, S., Cesaro, L., Arrigoni, G., Salvi, M. and Pinna, L.A. (2017) Exploring the CK2 paradox: restless, dangerous, dispensable. *Pharmaceuticals (Basel)*, **10**, 11.
- Helm, S., Dobritsch, D., Rodiger, A., Agne, B. and Baginsky, S. (2014) Protein identification and quantification by data-independent acquisition and multi-parallel collision-induced dissociation mass spectrometry (MS(E)) in the chloroplast stroma proteome. *J. Proteomics*, **98**, 79–89.
- Hooper, C.M., Castleden, I., Tanz, S.K., Aryamanesh, N. and Millar, A.H. (2017) SUBA4: the interactive data analysis centre for Arabidopsis sub-cellular protein locations. *Nucleic Acids Res.* **45**, D1064–D1074.
- Howard, T.P., Fryer, M.J., Singh, P. *et al.* (2011) Antisense suppression of the small chloroplast protein CP12 in tobacco alters carbon partitioning and severely restricts growth. *Plant Physiol.* **157**, 620–631.

- Kim, S.Y., Bender, K.W., Walker, B.J., Zielinski, R.E., Spalding, M.H., Ort, D.R. and Huber, S.C. (2016) The plastid casein kinase 2 phosphorylates rubisco activase at the Thr-78 site but is not essential for regulation of rubisco activation state. *Front. Plant Sci.* **7**, 404.
- Koskela, M.M., Brünje, A., Ivanauskaite, A. et al. (2018) Chloroplast acetyltransferase NSI is required for state transitions in *Arabidopsis thaliana*. *Plant Cell*, **30**, 1695–1709.
- Lisec, J., Schauer, N., Kopka, J., Willmitzer, L. and Fernie, A.R. (2006) Gas chromatography mass spectrometry-based metabolite profiling in plants. *Nat. Protoc.* **1**, 387–396.
- Lolli, G., Naressi, D., Sarno, S. and Battistutta, R. (2017) Characterization of the oligomeric states of the CK2 alpha2beta2 holoenzyme in solution. *Biochem. J.* **474**, 2405–2416.
- Luedemann, A., Strassburg, K., Erban, A. and Kopka, J. (2008) TagFinder for the quantitative analysis of gas chromatography–mass spectrometry (GC-MS)-based metabolite profiling experiments. *Bioinformatics*, **24**(5), 732–737. <http://dx.doi.org/10.1093/bioinformatics/btn023>.
- Lunde, C., Jensen, P.E., Haldrup, A., Knoetzel, J. and Scheller, H.V. (2000) The PSI-H subunit of photosystem I is essential for state transitions in plant photosynthesis. *Nature*, **408**, 613–615.
- Mulekar, J.J. and Huq, E. (2015) Arabidopsis casein kinase 2 alpha4 subunit regulates various developmental pathways in a functionally overlapping manner. *Plant Sci.* **236**, 295–303.
- Pinna, L.A. (2002) Protein kinase CK2: a challenge to canons. *J. Cell Sci.* **115**, 3873–3878.
- Reiland, S., Messerli, G., Baerenfaller, K., Gerrits, B., Endler, A., Grossmann, J., Gruissem, W. and Baginsky, S. (2009) Large-scale Arabidopsis phosphoproteome profiling reveals novel chloroplast kinase substrates and phosphorylation networks. *Plant Physiol.* **150**, 889–903.
- Rochaix, J.D. (2014) Regulation and dynamics of the light-harvesting system. *Annu. Rev. Plant Biol.* **65**, 287–309.
- Rocha, A.G., Mehlmer, N., Stael, S., Mair, A., Parvin, N., Chigri, F., Teige, M. and Voithknecht, U.C. (2014) Phosphorylation of Arabidopsis transketolase at Ser428 provides a potential paradigm for the metabolic control of chloroplast carbon metabolism. *Biochem. J.* **458**, 313–322.
- Rusin, S.F., Adamo, M.E. and Kettenbach, A.N. (2017) Identification of candidate casein kinase 2 substrates in mitosis by quantitative phosphoproteomics. *Front. Cell Dev. Biol.* **5**, 97.
- Salinas, P., Fuentes, D., Vidal, E., Jordana, X., Echeverria, M. and Holuigue, L. (2006) An extensive survey of CK2 alpha and beta subunits in Arabidopsis: multiple isoforms exhibit differential subcellular localization. *Plant Cell Physiol.* **47**, 1295–1308.
- Salvi, M., Sarno, S., Cesaro, L., Nakamura, H. and Pinna, L.A. (2009) Extraordinary pleiotropy of protein kinase CK2 revealed by weblogo phosphoproteome analysis. *Biochim. Biophys. Acta*, **1793**, 847–859.
- Sarno, S. and Pinna, L.A. (2008) Protein kinase CK2 as a druggable target. *Mol. Biosyst.* **4**, 889–894.
- Schmidt, O., Harbauer, A.B., Rao, S. et al. (2011) Regulation of mitochondrial protein import by cytosolic kinases. *Cell*, **144**, 227–239.
- Schönberg, A., Bergner, E., Helm, S., Agne, B., Dünschede, B., Schöne-mann, D., Schutkowski, M. and Baginsky, S. (2014) The peptide microarray "ChloroPhos1.0" identifies new phosphorylation targets of plastid casein kinase II (pCKII) in *Arabidopsis thaliana*. *PLoS One*, **9**, e108344.
- Schönberg, A., Rödiger, A., Mehwald, W., Galonska, J., Christ, G., Helm, S., Thieme, D., Majovsky, P., Hoehenwarter, W. and Baginsky, S. (2017) Identification of STN7/STN8 kinase targets reveals connections between electron transport, metabolism and gene expression. *Plant J.* **90**, 1176–1186.
- Siddiqui-Jain, A., Bliesath, J., Macalino, D. et al. (2012) CK2 inhibitor CX-4945 suppresses DNA repair response triggered by DNA-targeted anti-cancer drugs and augments efficacy: mechanistic rationale for drug combination therapy. *Mol. Cancer Ther.* **11**, 994–1005.
- Solimini, N.L., Luo, J. and Elledge, S.J. (2007) Non-oncogene addiction and the stress phenotype of cancer cells. *Cell*, **130**, 986–988.
- Stanley, D.N., Raines, C.A. and Kerfeld, C.A. (2013) Comparative analysis of 126 cyanobacterial genomes reveals evidence of functional diversity among homologs of the redox-regulated CP12 protein. *Plant Physiol.* **161**, 824–835.
- St-Denis, N., Gabriel, M., Turowec, J.P., Gloor, G.B., Li, S.-S.-C., Gingras, A.-C. and Litchfield, D.W. (2015) Systematic investigation of hierarchical phosphorylation by protein kinase CK2. *J. Proteomics*, **118**, 49–62.
- Trotta, A., Bajwa, A.A., Mancini, I., Paakkarinen, V., Pribil, M. and Aro, E.M. (2019) The role of phosphorylation dynamics of curvature thylakoid 1B in plant thylakoid membranes. *Plant Physiol.* **181**, 1615–1631.
- Turkeri, H., Schweer, J. and Link, G. (2012) Phylogenetic and functional features of the plastid transcription kinase cpCK2 from Arabidopsis signify a role of cysteinyl SH-groups in regulatory phosphorylation of plastid sigma factors. *Febs J.* **279**, 395–409.
- Tyanova, S., Temu, T. and Cox, J. (2016) The MaxQuant computational platform for mass spectrometry-based shotgun proteomics. *Nat. Protoc.* **11**, 2301–2319.
- Vilk, G., Weber, J.E., Turowec, J.P. et al. (2008) Protein kinase CK2 catalyzes tyrosine phosphorylation in mammalian cells. *Cell. Signal.* **20**, 1942–1951.
- Wagner, R., Dietzel, L., Bräutigam, K., Fischer, W. and Pfannschmidt, T. (2008) The long-term response to fluctuating light quality is an important and distinct light acclimation mechanism that supports survival of *Arabidopsis thaliana* under low light conditions. *Planta*, **228**, 573–587.
- Wang, Y., Chang, H., Hu, S. et al. (2014) Plastid casein kinase 2 knockout reduces abscisic acid (ABA) sensitivity, thermotolerance, and expression of ABA- and heat-stress-responsive nuclear genes. *J. Exp. Bot.* **65**, 4159–4175.
- Wang, W.S., Zhu, J., Zhang, K.X., Lü, Y.T. and Xu, H.H. (2016) A mutation of casein kinase 2 α 4 subunit affects multiple developmental processes in Arabidopsis. *Plant Cell Rep.* **35**, 1071–1080.
- Wessel, D. and Flugge, U.I. (1984) A method for the quantitative recovery of protein in dilute solution in the presence of detergents and lipids. *Anal. Biochem.* **138**, 141–143.
- Yu, Q.B., Zhao, T.T., Ye, L.S., Cheng, L., Wu, Y.Q., Huang, C. and Yang, Z.N. (2018) pTAC10, an S1-domain-containing component of the transcriptionally active chromosome complex, is essential for plastid gene expression in *Arabidopsis thaliana* and is phosphorylated by chloroplast-targeted casein kinase II. *Photosynth. Res.* **137**, 69–83.